Transfection kit (Pharmingen). In each case the recombinant extracellular virus (rECV) was purified by a limiting dilution dot-blot hybridization procedure (*16*). The cells were infected at 80% confluence with rECV at a multiplicity of infection of 10 and harvested typically 72 hours after infection. For purification of recombinant GST-α_T, frozen cell pellets were thawed and resuspended in HMDN buffer [20 mM Hepes (pH 7.4), 5 mM $MgCl_2$, 1 mM dithiothreitol (DTT), and 100 mM NaCl] containing Triton X-100 (1%) or cholate (1%) and the protease inhibitors aprotinin and leupeptin. Cells were lysed by sonication on ice, the lysates were centrifuged at 40,000*g*, and sedimented material was discarded. The soluble GST fusion proteins were purified by glutathione-agarose affinity chromatography. Purified proteins were dialysed against HMDN buffer (pH 7.4) before use in assays. The protease thrombin was used (at a fusion protein:protease ratio of 50:1) to separate the GST and α_T proteins by cutting at a thrombin recognition site. Digestion was done in HMDN buffer supplemented with 2.5 mM $CaCl_2$, at 4°C for 3 hours. Liberated GST subunits and undigested GST-α_T were removed by glutathione-agarose affinity chromatography to yield purified wild-type α_T and α_TE203A.

8. C. Van Dop *et al.*, *J. Biol. Chem.* **259**, 23 (1984).
9. T. Higashijima *et al.*, *ibid.* **262**, 752 (1987).
10. T. Higashijima, K. M. Ferguson, M. D. Smigel, A. G. Gilman, *ibid.*, p. 757.
11. W. J. Phillips and R. A. Cerione, *ibid.* **263**, 15498 (1988).
12. P. M. Guy, J. G. Koland, R. A. Cerione, *Biochemistry* **29**, 6954 (1990).
13. R. Mittal *et al.*, unpublished results.
14. H. M. Rarick, O. Artemyer, H. E. Hamm, *Science* **256**, 1031 (1992).
15. N. O. Artemyer, H. M. Rarick, J. S. Mills, N. P. Skiba, H. E. Hamm, *J. Biol. Chem.* **267**, 25067 (1992).
16. B. B. Goswami and R. I. Glazer, *Biotechniques* **5**, 626 (1991).

17. The GTPase activities of retinal α_T and the recombinant α_T subunits were measured as described (*12*). Briefly, the individual proteins (100 nM α_T, 100 nM retinal $\beta\gamma_T$) and phosphatidylcholine vesicles containing rhodopsin (*12*) were assayed for 10 min in a total volume of 200 μl at room temperature. The reactions were done in 20 mM sodium Hepes (pH 7.4), 5 mM $MgCl_2$, 1 mM DTT, and 100 mM NaCl and were initiated by the addition of GTP and [γ-^{32}P]GTP to a final concentration of 1 μM. After 10 min, the reactions were quenched by the addition of 5 ml of 10% ammonium molybdate solution. The [γ-^{32}P]P_i released upon GTP hydrolysis was extracted by the addition of 5 ml of a 1:1 mixture of isobutanol and benzene and quantitated by liquid scintillation counting. Background hydrolysis of GTP was measured by quantitating P_i release by rhodopsin-containing lipid vesicles and $\beta\gamma$T without added α_T-GDP, or by measuring the GTPase activity by α_T-GDP with $\beta\gamma_T$ in the absence of rhodopsin-containing lipid vesicles.

18. R. Yee and P. A. Liebman, *J. Biol. Chem.* **253**, 8902 (1978).

19. The GTP-γ-S–binding activities of retinal α_T and recombinant α_T subunits were measured in a manner similar to the GTPase assays (*17*). Reactions were initiated by the addition of a mixture of GTP-γ-S and [^{35}S]GTP-γ-S to a final concentration of 1 μM. The reaction mixtures were incubated for 20 min at room temperature, then quenched by the addition of ice-cold buffer containing 20 mM sodium Hepes (pH 7.4), 5 mM $MgCl_2$, and 100 mM NaCl, and then added to 0.45-μm nitrocellulose filters on a suction manifold. The filters were washed twice with 3 ml of buffer and counted in 3 ml of Liquiscient (National Diagnostics). Nonspecific binding was determined by measuring [^{35}S]GTP-γ-S binding to α_T-GDP with $\beta\gamma_T$ in the presence of lipid vesicles that lacked rhodopsin, or by measuring binding to $\beta\gamma_T$- and rhodopsin-containing lipid vesicles in the absence of added α_T-GDP.
20. Pertussis toxin–catalyzed ADP ribosylation was performed by incubating the α_T subunits (2 μg) with lipid vesicles lacking rhodopsin (*12*) and various amounts of the $\beta\gamma_T$ subunit complex (0 to 2 μg) at room temperature in a total volume of 40 μl in the presence of 250 ng of activated pertussis toxin, 1.25 μM nicotinamide adenine dinucleotide (NAD), 0.5 μCi per assay of [α-^{32}P]NAD, 50 mM tris-Cl (pH 8.0), 3 mM $MgCl_2$, 1 mM DTT, 50 μM GTP, and 0.5 mM adenosine triphosphate. The reactions were incubated for 1 hour at room temperature and then Laemmli sample buffer was added and the samples subjected to SDS–polyacrylamide gel electrophoresis (PAGE) and autoradiography.
21. Measurements of cyclic GMP (cGMP) hydrolysis by the retinal cGMP-dependent PDE were done as described (*18*). Briefly, a pH microelectrode was used to measure the decrease in pH that resulted from the production of one proton for each molecule of cGMP hydrolyzed by the PDE. All assays were done at room temperature in a final volume of 200 μl in a buffer containing 5 mM Hepes (pH 8.0), 5 mM $MgCl_2$, and 100 mM NaCl. All PDE assays contained 10 pmol of intact holoPDE and when measuring the GTP-γ-S–bound α_T-stimulated activity, 15 pmol of the α_T–GTP-γ-S complex. Loading of the α_T subunits with GTP-γ-S was done with rhodopsin that had been reconstituted into phosphatidylcholine vesicles and purified retinal $\beta\gamma_T$ (*12*). Equivalent amounts of the different α_T subunits, as quantitated by [^{35}S]GTP-γ-S binding (*12*), were added to the PDE assays. The PDE assays were initiated by the addition of cGMP to a final concentration of 5 mM, and the change in pH (in millivolts) was measured once per second. At the end of the assay period (~200 s), the buffering capacity (millivolts per nanomole) was determined by the addition of 0.1 μmol of KOH to the reaction mixture. The rate of hydrolysis of cGMP (nanomoles per second) was determined from the ratio of the slope of the pH record (millivolts per second) and the buffering capacity of the assay buffer (millivolts per nanomole).

22. We thank J. V. Platko for discussions and molecular biological advice and C. Westmiller for technical assistance. Supported by grants from NIH.

2 October 1995; accepted 19 December 1995

Rearrangement-Enhancing Element Upstream of the Mouse Immunoglobulin Kappa Chain J Cluster

Laurent Ferradini,* Hua Gu,† Annie De Smet, Klaus Rajewsky, Claude-Agnès Reynaud, Jean-Claude Weill

Transcriptional regulatory elements have been shown to be necessary but not sufficient for the developmental regulation of immunoglobulin gene rearrangement in mouse precursor B cells. In the chicken λ light chain locus, additional elements in the V-J intervening sequence are involved in negative and positive regulation of rearrangement. Here, mutation of the mouse homolog of a chicken element, located in the V_κ-J_κ intervening sequence upstream of the J_κ cluster, was shown to significantly decrease rearrangement. This cis-acting recombination-enhancing element affects the rearrangement process without being involved in regulating transcription.

During differentiation in the bone marrow, most B cell precursors undergo successive rounds of immunoglobulin (Ig) gene rearrangement: D-J then V-DJ joining for the heavy chain, followed by V-J joining for the light chains (*1*, *2*). Because the same recombinase machinery is involved at each stage, specific elements are thought to account for such a developmental regulation by controlling the accessibility of the loci (*3*). Experiments with transgenic recombination substrates as well as homologous recombination have shown that transcriptional regulatory elements are necessary for these events to occur (*4*–*6*).

Using a chicken λ light chain transgene in its natural germline configuration, we previously showed that, in addition to the enhancer and promoter, other elements located in the V-J intervening sequence regulate rearrangement of this locus in mouse pre-B cells (*6*, *7*). One of these additional elements reduces rearrangement, hence we call it a "silencer." The silencer is flanked by one element (or possibly two) counteracting its effect, hence we call it an "antisilencer" (*6*). We proposed that the silencer and antisilencer are involved in ensuring allelic exclusion at the chicken λ locus (*8*). One of the chicken antisilencer elements is homologous in sequence and location to two palindromic motifs (called KI and KII) located in the mouse V_κ-J_κ intervening sequence upstream of the J_κ1 gene segment and previously described as binding sites for a factor present in mouse pre-B and B cells (*9*).

To investigate the role of the KI and KII sites in regulating mouse κ light chain rearrangement, we generated KI-KII mutant mice using the gene-targeting method in mouse embryonic stem (ES) cells (*10*). The vector used for transfection contained a murine J_κ genomic fragment (*11*) in which the KI and KII sites were altered by site-directed mutagenesis to replace 8 and 9 base pairs (bp) of the KI and KII sites, respectively, in order to modify the overall structure of these sites (Fig. 1A). In addition, we used the Cre-*lox*P system of bacteriophage

L. Ferradini, A. De Smet, C.-A. Reynaud, J.-C. Weill, INSERM U373, Institut Necker, Faculté de Médecine Necker-Enfants Malades, Université Paris V, 156 rue de Vaugirard, 75730 Paris Cedex 05, France.
H. Gu and K. Rajewsky, Institut für Genetik, Universität Köln, Weyertal 121, D-50931 Köln, Germany.

*To whom correspondence should be addressed.
†Present address: Laboratory of Immunology, National Institute of Allergy and Infectious Diseases, National Institutes of Health, 12441 Parklawn Drive, Rockville, MD 20852, USA.

P1 (*12, 13*) (Fig. 1B) to delete the neomycin resistance gene (*neo*^{r}) in order that a transcriptionally active *neo*^{r} gene, which could interfere with the regulation of rearrangement, did not remain in the targeted locus. At the 5′ end of the genomic sequence, we introduced the herpes simplex virus thymidine kinase gene (HSV-*tk*) to allow selection against random integration (Fig. 1B) (*14, 15*).

The linearized vector was electroporated into E14.1 ES cells (*16, 17*). After double selection with G418 and ganciclovir (*15*), the surviving clones were screened by Southern (DNA) blot analysis to verify the structure of the targeted locus on both sides and the presence of the KI and KII mutations (*18*). In a second step, independently targeted clones were transiently transfected with a Cre-recombinase–expressing vector to delete the *neo*^{r} gene from the locus (*12, 13, 16*). After appropriate selection, the deleted clones were identified by Southern blot analysis (*18*). Some clones had recombined between the *neo*^{r} gene and the KI-KII mutations during the targeting event (*19*); these clones were used to control that the *lox*P site remaining in the locus after the deletion of the *neo*^{r} gene does not affect rearrangement. Cells from three independently mutated clones and one *lox*P control clone were injected into severe combined immunodeficiency disease (SCID) and C57BL/6 blastocysts; the resulting chimeras were mated with CB20 and C57BL/6 mice, respectively, for germline transmission of the mutations.

We investigated the influence of the KI-KII mutations on rearrangement in the SCID chimeric mice because all their peripheral lymphoid cells are derived from the injected ES cells. Sorted splenic B and T cells were analyzed by Southern blot with the diagnostic restriction enzymes (Fig. 1B). As the diagnostic sites in the KI and KII elements are lost upon rearrangement, mutant versus wild-type alleles can only be discriminated when the κ loci are unrearranged, that is, in the germline configuration. The proportion of DNA remaining in the germline configuration in B cells for each allele is therefore used to estimate their relative rearrangement frequencies. As seen in Fig. 2, the intensity of the wild-type germline band was much less than the mutant one in B cells, whereas both alleles gave bands of comparable intensity in T cells. We conclude that rearrangement in pre-B cells from these SCID chimeric mice takes place mostly on the wild-type allele. The analysis of several chimeras, as well as heterozygous mice representing altogether three independent ES clones, yielded similar results (*18*).

The reduction in rearrangement seen on the Southern blots was confirmed with a polymerase chain reaction (PCR) strategy to amplify the genomic DNA surrounding the KI-KII mutations. The amplified product was digested with Sph I or Xba I or both to estimate the ratio of wild-type (Sph I–digested) to mutated (Xba I–digested) germ-

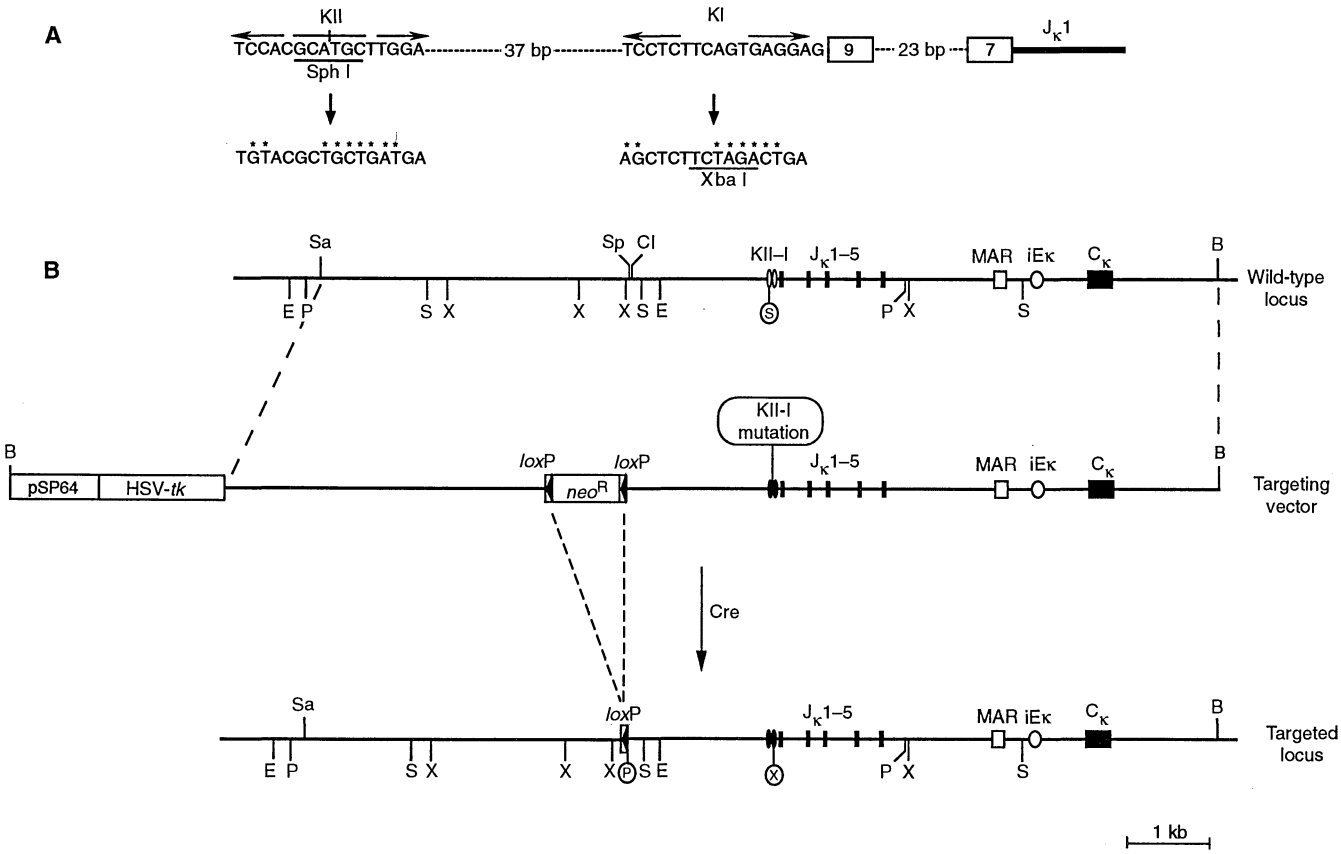

Fig. 1. (**A**) Mutations of the mouse KI and KII sites. The mutations were introduced by directed mutagenesis and verified by sequencing. Modified nucleotides are shown by stars. The palindromic structure of both sites (noted by horizontal arrows) was destroyed. To aid in analysis, the Sph I site in the wild-type KII sequence was destroyed and a new Xba I site was introduced in the mutant KI sequence. The heptamer and nonamer sequences of the recombination signal sequence are represented by boxes and the $J_\kappa1$ gene segment by a bold line. (**B**) Gene-targeting of the murine J_κ locus. The targeting vector contains the 11.5-kb Sal I–Bam HI fragment of the J_κ locus, which includes the KI-KII mutation, the elements $J_\kappa1$ to $J_\kappa5$ ($J_\kappa1$–5), the J-C intervening sequence, and the C_κ gene (*11*). The *neo*^{r} gene flanked by *lox*P sites was introduced 2 kb upstream of $J_\kappa1$, and the HSV-*tk* gene flanked by the pSP64 plasmid was positioned at the 5′ end of the Bam HI linearized construct (*14, 15*). The vector was introduced by electroporation into ES cells (*16*). In a second step, the *neo*^{r} gene was deleted (small dashed lines) from the targeted locus by transient transfection of the targeted clones with a Cre-recombinase–expressing plasmid (*16*). The remaining *lox*P site is shown, and the diagnostic enzyme restriction sites are circled. E, Eco RV; B, Bam HI; S, Sph I; X, Xba I; P, Pst I; Sa, Sal I; Sp, Spe I; Cl, Cla I; MAR, matrix attachment region; iEκ, intronic enhancer kappa.

line DNA in the samples studied (Fig. 3A). In sorted splenic T and B cells from SCID chimeras, as well as from a heterozygous mouse, the wild-type amplified fragment was drastically reduced compared to the mutant fragment in B cells, but not in T or the corresponding ES cells (Fig. 3B). As can be seen from the phosphorimager quantification of the results obtained with this PCR assay and shown in Table 1, in B cells from mutant mice about 10 and 90% of the PCR products correspond to wild-type and mutant alleles, respectively; these PCR products are distributed equally for both alleles in the corresponding T and ES cells. These results suggest that rearrangement of the mutant allele is reduced by about 80%. Such a quantification might even underestimate the reduction of rearrangement because the amount of wild-type germline DNA detected in our assay could have been increased by contaminating nonlymphoid cells (less than 2% in each case studied) or by κ-expressing B cells that have rearranged by inversion involving the gene segments $J_\kappa 3$ to $J_\kappa 5$. However, similar quantitative results were obtained from Southern blot analysis (*18*) in which such inversions were not taken into account. Altogether, the Southern blot (Fig. 1) and the PCR analysis indicated that the KI-KII mutations reduce rearrangement considerably (~80%), but that the block is not complete.

As the Cre-induced *neo*^{r} gene deletion leaves a *lox*P site about 2 kb upstream of $J_\kappa 1$, we analyzed a chimera obtained from a *lox*P control clone containing the remaining *lox*P site but not the KI-KII mutations. B cells of the *lox*P control chimera were sorted for the ES-derived allotype, and DNA surrounding the site of *lox*P integration was amplified. Both *lox*P-containing and wild-type alleles were amplified to a similar extent (*18*); thus, the *lox*P site does not by itself affect rearrangement appreciably.

To our surprise, heterozygous and homozygous mice for the KI-KII mutations were found to have peripheral B cells in normal numbers with an unmodified κ/λ ratio. This was true even when young mice (2- to 3-week-old) were analyzed (*18*, *20*). A four-color analysis of bone marrow cells showed that pro-B, pre-B, and immature B cells are represented in apparently normal proportions in 4- to 6-week-old heterozygous and homozygous mice (*18*, *21*); thus, despite the presence of the mutation, normal pre-B cell development seems to occur in these mice. As $J_\kappa 1$ is the most frequently used J_κ gene segment during rearrangement in primary B cells (*22*), it was suggested that the KI-KII elements, located just upstream of $J_\kappa 1$, could target the recombinase to this gene segment (9). However, a similar pattern of J_κ usage was detected by PCR in peripheral B cells from wild-type and homozygous mice (*18*); that is, the KI-KII mutation does not selectively reduce the frequency of $J_\kappa 1$ rearrangement.

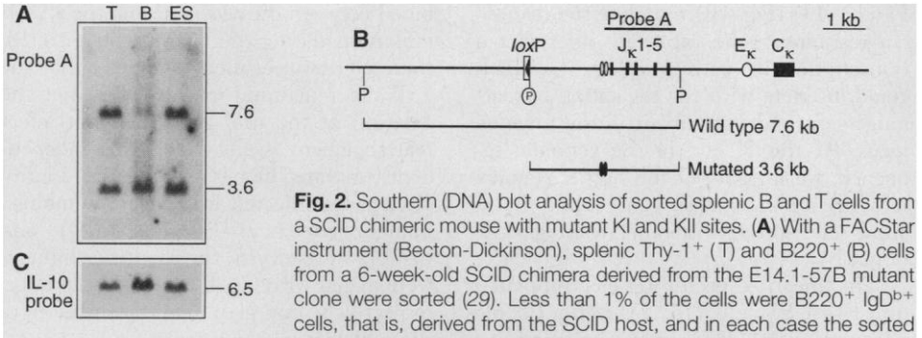

Fig. 2. Southern (DNA) blot analysis of sorted splenic B and T cells from a SCID chimeric mouse with mutant KI and KII sites. (**A**) With a FACStar instrument (Becton-Dickinson), splenic Thy-1$^+$ (T) and B220$^+$ (B) cells from a 6-week-old SCID chimera derived from the E14.1-57B mutant clone were sorted (*29*). Less than 1% of the cells were B220$^+$ IgD^{b+} cells, that is, derived from the SCID host, and in each case the sorted cells were ~98% pure (*18*). Genomic DNA from B, T, and the original E14-57B ES clone was digested with Pst I and analyzed by Southern blotting with the probe A. (**B**) The restriction map of the mutant Ig_κ locus with the expected germline Pst I (P) restriction fragments corresponding to the wild-type and the mutant loci. (**C**) The blot in (A) rehybridized with an interleukin-10 gene probe (*30*), to serve as a control (6.5-kb Pst I fragment).

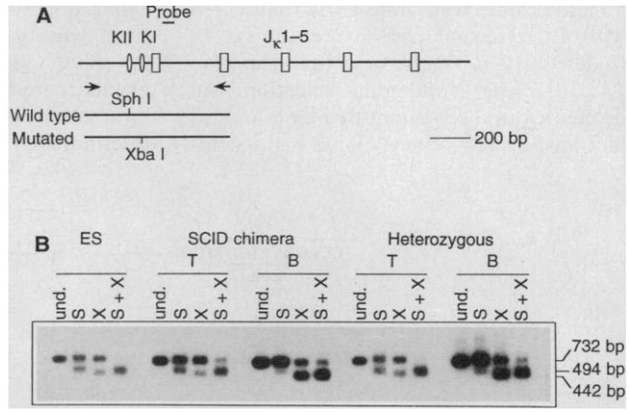

Fig. 3. PCR analysis of the J_κ germline locus from sorted splenic B and T cells of a SCID chimeric mouse and a heterozygous mouse with mutant KI and KII sites. (**A**) Strategy used to amplify J_κ genomic DNA. Primers (5′ primer: 5′-GAACTGCAGTCCTATGGAAGAGCAGCGAGTGCC-3′; 3′ $J_\kappa 2$ primer: 5′-CCAAGCTTTCCAGCTTGGTCCCCCCTCCGAA-3′) were chosen for amplification of a 0.7-kb fragment encompassing the KI and KII sites (*31*). PCR products of the correct size were gel purified and reanalyzed after digestion with Sph I, Xba I, or both to distinguish wild-type (Sph I–digested) from mutant (Xba I–digested) amplified products. An oligonucleotide (5′-GACATAGAAGCCACAGACATAGACAACGG-3′), hybridizing between $J_\kappa 1$ and $J_\kappa 2$, was used as a probe for Southern blot analysis. (**B**) Southern blot analysis of the amplified J_κ genomic DNA of sorted splenic B and T cells from a SCID chimera and a heterozygous mouse. Cells were sorted as in Fig. 2 (*29*). The 732-bp band corresponds to undigested amplified material, whereas the 494-bp band corresponds to Sph I– and the 442-bp band to Xba I–digested material. About 5 to 10% of the PCR product was not digested by either enzyme and probably reflects the presence of hybrid molecules. Und., undigested; S, digested with Sph I; and X, digested with Xba I.

Germline transcription of immunoglobulin (Ig) gene segments appears to be correlated with rearrangement during B cell development, and it is thought that transcription plays a role in the rearrangement process (*1*, *23*). For the κ locus, two distinct types of transcripts initiating approximately 3.5 and 0.1 kb upstream of $J_\kappa 1$ have been reported (*24*, *25*). As several initiation sites for the shortest transcripts are within the KI and the KII sequences, they might have been modified by the mutation we introduced. Transcripts initiating within KII were analyzed by reverse transcriptase (RT)–PCR in bone marrow B220$^+$ IgM$^-$ B cell precursors from mutant mice. We found that both alleles were transcribed similarly in heterozygous animals (Fig. 4). Although only one type of germline transcript can be detected in our assay, its presence indicates that, despite the KI-KII mutations, the J_κ locus is accessible to the transcriptional machinery. To find out whether the KI-KII mutations impair accessibility to the recombinase by modulating methylation, we used the previous PCR strategy (Fig. 3) to test the methylation status of the J_κ locus in fractions of bone marrow cells from heterozygous mice (*26*). The results showed no obvious difference in methylation between the wild-type and the mutant allele (*18*).

In conclusion, the KI-KII mutation acts in cis to decrease considerably V_κ-J_κ rearrangement, but it does not prevent accessibility to the locus, as monitored by the germline transcription, the methylation status, and the baseline amount of rearrangement, which are maintained on the mutant allele (*27*). This baseline amount of rearrangement is compatible with normal B cell

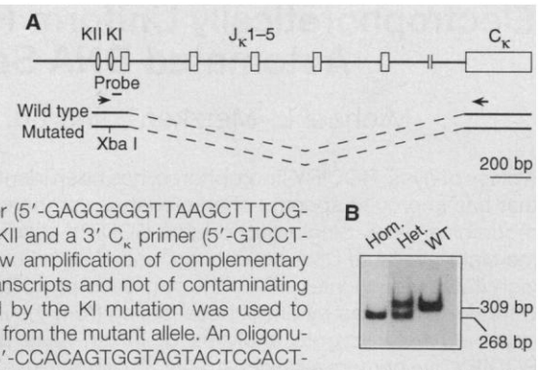

Fig. 4. RT-PCR analysis of κ germline transcripts in B220$^+$ IgM$^-$ bone marrow B cell precursors from heterozygous and homozygous mice. (**A**) Short germline transcripts from the wild-type and the mutated alleles are represented. Primers, shown above the transcripts, were designed to amplify transcripts initiating within KII, with a 5′ primer (5′-GAGGGGGTTAAGCTTTCGCAGCTACC-3′) located between KI and KII and a 3′ C_κ primer (5′-GTCCTGATCAGTCCAACTGTTCAG-3′) that allow amplification of complementary DNA (cDNA) corresponding to spliced transcripts and not of contaminating germline DNA. The Xba I site introduced by the KI mutation was used to distinguish germline transcripts originating from the mutant allele. An oligonucleotide hybridizing just upstream of J_κ1 (5′-CCACAGTGGTAGTACTCCACTGTCTGGCTG-3′) was used as a probe. (**B**) Southern blot analysis of RT-PCR products after digestion with Xba I. Total RNA from sorted bone marrow B220$^+$ IgM$^-$ B cell precursors (*29*) from homozygous (Hom.), heterozygous (Het.), and wild-type (WT) mice was prepared with RNAzol (Bioprobe Systems). First-strand cDNA synthesis (cDNA cycle kit, Invitrogen) was performed with random oligonucleotides. PCR products were gel-purified, digested with Xba I, and then separated on 6% acrylamide gel before electrotransfer and hybridization.

Table 1. Quantification of PCR amplification of wild-type and mutant germline J_κ alleles. Analysis of mice derived from two distinct targeted ES clones, E14-57B and E14-34D, is shown. Sorted B and T cells were obtained as in Fig. 2 from an E14-57B SCID chimera and a heterozygous mouse. The ES-derived splenic B cells from E14-34D B6 chimeras were sorted according to the IgD^a allotype (*29*). PCR analysis was performed as in Fig. 3 and quantified with a phosphorimager (Molecular Dynamics). The total amplified product minus hybrid products not digested by either Sph I or Xba I is defined as 100%.

J_κ allele	Percent of PCR products corresponding to a J_κ allele						
	ES	E14-57B ES clone				E14-34D ES clone	
		SCID chimera		Heterozygous		B6 chimera 1	B6 chimera 2
		T	B	T	B	B	B
Wild type	49	52.5	10	48.5	12	13.5	11
Mutant	51	47.5	90	51.5	88	86.5	89

development, resulting in no obvious alterations of the bone marrow B cell fractions or the κ/λ ratio in both heterozygous and homozygous animals. The influence of the KI-KII mutation is thus manifest in a context of competition between a mutant and a wild-type allele. The results presented here demonstrate the existence of a cis-acting recombination-enhancing sequence that affects Ig gene rearrangement process without being involved in regulating transcription. That is, while transcriptional regulatory elements (promoter and enhancer) are required to initiate rearrangement by inducing a change in chromatin structure and rendering DNA accessible to the recombinase, other elements including KI-KII participate in the regulation of rearrangement.

Taking into account the homology of the sequences between the chicken and mouse KI-KII sites, as well as the similar inhibition of rearrangement observed when these sites are mutated, we propose that the mouse element, like that of the chicken λ locus, is an antisilencer counterbalancing an upstream silencer element. Such a silencer-antisilencer couple present in the mouse V_κ-J_κ intervening sequence may provide the molecular basis for the two specific regulatory events required to achieve allelic exclusion during lymphoid development: the limited access to one allele that occurs during the onset of rearrangement and the feedback inhibition on the unrearranged allele once a productive rearrangement has been performed.

REFERENCES AND NOTES

1. G. D. Yancopoulos and F. W. Alt, *Cell* **40**, 271 (1985).
2. F. W. Alt, N. Rosenberg, S. Lewis, E. Thomas, D. Baltimore, *ibid.* **27**, 381 (1981).
3. G. D. Yancopoulos, T. K. Blackwell, H. Suh, L. Hood, F. W. Alt, *ibid.* **44**, 251 (1986); D. G. Schatz, M. A. Oettinger, D. Baltimore, *ibid.* **59**, 1035 (1989); M. A. Oettinger, D. G. Schatz, C. Gorka, D. Baltimore, *Science* **248**, 1517 (1990).
4. P. Ferrier *et al.*, *EMBO J.* **9**, 117 (1990); S. Takeda *et al.*, *ibid.* **12**, 2329 (1993).
5. M. Serwe and F. Sablitzky, *ibid.* **12**, 2321 (1993); J. Chen *et al.*, *ibid.*, p. 4635.
6. R. Lauster *et al.*, *ibid.*, p. 4615.
7. D. Bucchini *et al.*, *Nature* **326**, 409 (1987).
8. L. Ferradini, C.-A. Reynaud, R. Lauster, J.-C. Weill, *Semin. Immunol.* **6**, 165 (1994).
9. D. Weaver and D. Baltimore, *Proc. Natl. Acad. Sci. U.S.A.* **84**, 1516 (1987).
10. M. R. Capecchi, *Science* **244**, 1288 (1989).
11. The pSPlg8 plasmid containing the 12.7-kb Bam HI genomic New Zealand black mice DNA including the J_κ locus was provided by B. Van Ness (*24*).
12. N. Sternberg and D. Hamilton, *J. Mol. Biol.* **150**, 467 (1981); B. Sauer and N. Henderson, *New Biol.* **2**, 441 (1990).
13. H. Gu, Y.-R. Zou, K. Rajewsky, *Cell* **73**, 1155 (1993).
14. The KI and KII sites were altered by site-directed mutagenesis (Bio-Rad) and verified by sequencing. The Sal I–Xba I fragment containing the *lox*P-flanked *neo*^{r} gene driven by a *tk* promoter was obtained from the pLZ-*neo*^{r} plasmid (H. Gu, unpublished data) and ligated into the Cla I–Spe I sites 2 kb upstream of J_κ1. The HSV-*tk* gene was obtained from the pIC19R plasmid (*15*) and ligated blunt-ended as a Cla I–Hind III fragment into the Sal I site of the pSPlg8 plasmid. The targeted vector was then linearized with Bam HI for transfection.
15. S. L. Mansour, K. R. Thomas, M. R. Capecchi, *Nature* **336**, 348 (1988).
16. E14.1 ES cells were cultured according to (*17*) and transfected with the linearized vector (30 μg/ml) as described (*15*). After double selection with G418 and ganciclovir, the surviving clones were expanded and screened by Southern blot analysis. Among the double-selected clones, 32% had undergone specific appropriate homologous recombination, but only 18% shared the KI-KII mutations, because some (14%) were also recombined between the *neo*^{r} gene and the KI-KII mutations and hence contained the *neo*^{r} gene with wild-type KI and KII sites (*19*). To delete the *neo*^{r} gene, 10^7 targeted ES cells were transfected with supercoiled plasmid DNA pIC-Cre (*13*) by electroporation according to D. Kitamura, J. Roes, R. Kühn, and K. Rajewsky [*Nature* **350**, 423 (1991)] and plated at low density. After 10 days, colonies were picked and divided into two parts to select for G418-sensitive clones, which were expanded and verified for *neo*^{r} gene deletion by Southern blot analysis.
17. R. Kühn, K. Rajewsky, W. Müller, *Science* **254**, 707 (1991).
18. L. Ferradini *et al.*, data not shown.
19. C. Deng, K. R. Thomas, M. R. Capecchi, *Mol. Cell. Biol.* **13**, 2134 (1993).
20. No significant difference in the absolute numbers of B cells, calculated on viable nucleated splenocytes, was observed between 2-week-old homozygous [3.95 (±0.9) × 10^7, n = 7], heterozygous [3.86 (±0.25) × 10^7, n = 8], and wild-type [4.3 (±0.44) × 10^7, n = 5] mice from the same litter. The κ/λ ratio was analyzed on peripheral blood lymphocytes from 4-week-old mice stained with phycoerythrin (PE)–coupled antibody to B220 (anti-B220) and fluorescein isothiocyanate (FITC)–coupled anti-κ or anti-λ1 monoclonal antibodies (*29*). The percent of κ-expressing cells among B220$^+$ cells from CB20 homozygous mutant mice was 93.6 ± 0.9% (n = 7) compared with 93.45 ± 1.8% (n = 6) for wild-type mice from the same litter. In the same experiment, λ1-expressing B cells represented 2.19 ± 1% and 2.01 ± 0.55% of B220$^+$ cells in homozygous and wild-type mice, respectively. The κ/λ ratio was also found to be unchanged in newly generated bone marrow B cells (B220^{low}, μ$^+$) from 2-week-old mutant and wild-type mice.
21. Four-color staining was performed on cells from 4-week-old mice according to A. Ehlich *et al.* [*Cell* **72**, 695 (1993)] with antibodies against CD43/S7, heat-stable antigen (HSA), BP-1, and CD45R/B220 (*28*). Fractions A to C′ corresponding to pro-B cells were found to be present in wild-type (4.7 × 10^5 cells, n = 2), heterozygous (3.7 × 10^5 cells, n = 2), and homozygous (3.8 × 10^5 cells, n = 2) mutant mice. Fraction D corresponding to pre-B cells (B220$^+$ μ$^-$ S7$^-$), which are known to undergo κ chain rearrangement, was not enlarged in homozygous mutant mice (10.4 × 10^5 cells versus 13.3 × 10^5 in wild-type mice) and displayed a normal size distribution upon forward scatter analysis. However, with the PCR assay used in Fig. 3, the reduction in rearrangement on the mutant allele seen in spleen cells was already observed in bone marrow when looking at the fraction D in heterozygous mice (*18*). Fractions E (B220^{low} μ$^+$) and F (B220^{high} μ$^+$) corresponding to immature and mature B cells, respectively, were also represented in mutant mice. Similar results were obtained by analyzing bone marrow cells from 2-week-old mutant mice.
22. D. L. Wood and C. Coleclough, *Proc. Natl. Acad.*

Sci. U.S.A. **81**, 4756 (1984); M. Nishi, T. Kataoka, T. Honjo, *ibid.* **82**, 6399 (1985); C. A. Medina and J. M. Teale, *J. Exp. Med.* **177**, 1317 (1993).
23. T. K. Blackwell *et al. Nature* **324**, 585 (1986); F. W. Alt, T. K. Blackwell, G. D. Yancopoulos, *Science* **238**, 1079 (1987); M. S. Schlissel and D. Baltimore, *Cell* **58**, 1001 (1989).
24. B. G. Van Ness *Cell* **27**, 593 (1981).
25. L. Leclerc, P. Butkeraitis, M. Reth, *Nucleic Acid Res.* **17**, 6809 (1989); D. J. Martin and B. G. Van Ness, *Mol. Cell. Biol.* **10**, 1950 (1990).
26. The methylation status of the Hha I site located just upstream of the KI and KII sites [U. Storb and B. Arp, *Proc. Natl. Acad. Sci. U.S.A.* **80**, 6642 (1983); K. J. Nelson, E. L. Mather, R. P. Perry, *Nucleic Acids Res.* **12**, 1911 (1984)] was studied with the same PCR assay as the one described in Fig. 3. Bone marrow fractions C' and D, representing the cell populations engaged in the process of κ light chain rearrangement, were sorted from heterozygous animals (*21*) and the proportion of each allele assessed before and after Hha I (methylation-sensitive) digestion. No obvious difference in methylation between the wild-type and the mutant allele was observable in this assay (*18*).
27. These results differ from those obtained by Takeda *et al.* (*4*) with the intronic κ enhancer knock-out; in mice homozygous for that mutation, κ rearrangement is completely blocked. The total number of B cells in these mice was about half that in normal mice, and only λ-expressing B cells were detected in the periphery. Whether the deletion of the intronic κ enhancer is sufficient by itself to completely abolish accessibility and rearrangement remains an open question. The neomycin gene left in the κ locus at the site of the enhancer might by itself contribute to making the block of rearrangement observed in Takeda *et al.* complete (*4*). The sole insertion of the neomycin gene at the 3′ end of the enhancer also shows some inhibition (*4*). We note that in the knock-out experiments with the Igμ intronic enhancer, inhibition of rearrangement is much more profound when the neomycin gene is left in the locus (*5*). See also P. Artelt *et al.*, *Gene* **99**, 249 (1991), for a possible silencing effect of the neomycin gene.
28. R. R. Hardy, C. E. Carmack, S. A. Shinton, J. D. Kemp, K. Hayakawa, *J. Exp. Med.* **173**, 1213 (1991).
29. The following monoclonal antibodies were used for flow cytometric analysis: PE-conjugated RA3-6B2 [anti-CD45R/B220; R. L. Coffman, *Immunol. Rev.* **69**, 5 (1982)]; FITC-conjugated CFO-1 [anti-Thy1.2; H. G. Opitz, U. Opitz, G. Hewlett, H. D. Schlumberger, *Immunobiology* **160**, 438 (1982)]; R33-24-12 [anti-μ; R. Grützmann, thesis, University of Cologne, Cologne, Germany (1981)]; 4/4D7 (anti-δ^b; gift of T. Tokuhisa); 10-4-22 [anti-δ^a; V. T. Oi and L. A. Herzenberg, *Mol. Immunol.* **16**, 1005 (1979)]; R33-18 [anti-κ; R. Grützmann, thesis, University of Cologne, Cologne, Germany (1981)]; goat antibody to mouse λ (Southern Biotechnology Association); LS136 [anti-λ1; M. Reth, thesis, University of Cologne, Cologne, Germany (1981)]; S7 (anti-CD43/S7; provided by S. Kemp); and BP-1 and 30F1 [anti-HSA (*28*)].
30. R. Kühn, J. Löhler, D. Rennick, K. Rajewsky, W. Müller, *Cell* **75**, 263 (1993).
31. The 3′ primer has been previously described [M. S. Schlissel and D. Baltimore, *Cell* **58**, 1001 (1989)]. PCR amplification was performed in a volume of 50 μl in a Perkin-Elmer 9600 thermal cycler for 30 cycles. Each cycle consisted of 1 min at 94°C and 2 min at 72°C. The reaction buffer contained 10 mM tris-HCl (pH 8.3), 50 mM KCl, 1.5 mM $MgCl_2$, 200 μM of each deoxynucleotide triphosphate, 25 pmol of each primer, and 1 U of Taq polymerase (Perkin- Elmer).
32. We thank B. Van Ness for providing us the pSPlg8 plasmid; R. Kühn for the E14.1 ES clone; A. Egert for advice and technical help; C. Steinberg for helpful comments and critical reading of the manuscript; R. Torres, Y.-R. Zou, F. Huetz, and L. Quint for encouragements and discussions; J.-P. De Villartay for phosphorimager quantifications; S. Schaal for bone marrow analysis; and C. Garcia for cell sorting experiments. This work was partly supported by a short-term European Molecular Biology Organization fellowship.

21 June 1995; accepted 16 January 1996

Electrophoretically Uniform Fluorescent Dyes for Automated DNA Sequencing

Michael L. Metzker,* Jing Lu, Richard A. Gibbs

A class of dyes, BODIPY fluorophores, has been identified for automated DNA sequencing that has improved spectral characteristics compared with conventional fluorescein and rhodamine dyes. Single and double BODIPY dye primers were characterized in commercially available DNA sequencers and showed uniform electrophoretic mobilities and high fluorescence intensities. The improved physical properties of BODIPY dye primers were demonstrated by direct base-calling from the unprocessed fluorescent signals and improved heterozygote analyses of mixed-base populations. The high sensitivity of BODIPY dye primers requires at least 33 percent less reagent consumed per reaction than conventional dye primers, which should affect the costs of large genome-sequencing efforts.

Families of fluorescent dyes form the basis of multicomponent DNA detection assays. In automated DNA sequencing, up to four dyes are attached to oligonucleotides (*1*) that are enzymatically extended by DNA polymerase to generate a set of nested fragments. DNA sequence data are obtained after electrophoretic separation of the DNA and excitation, detection, and processing of the raw fluorescent signal by a computer. The generation and interpretation of these mixed fluorescent signals are therefore the central elements of current DNA sequencing technology.

Dyes suitable for high-throughput genome-scale DNA sequencing require the combined properties of physical stability, minimally overlapping emission spectra, high fluorescence intensity, and uniform electrophoretic mobilities. Although physically stable, the currently available set of fluoroscein and rhodamine dyes do not meet the remaining criteria and require both chemical and software corrections to produce optimal data (*1*).

Four spectrally resolvable dipyrromethene boron difluoride (BODIPY) dyes have been identified (Fig. 1) that show uniform electrophoretic properties under a variety of polyacrylamide gel conditions. Initially, the substitution of a BODIPY-labeled universal sequencing primer (Fig. 2A) for the same primer labeled with the corresponding fluorescein or rhodamine dye (*2*) generated termination reactions products that migrated approximately ¾ to 1 base faster by gel electrophoresis (Fig. 3, A and B). Substitution of BODIPY dyes labeled with various linker-arm modifications (Fig. 2A) revealed the optimal configurations that mimicked the mobility pattern of software-corrected fluorescein or rhodamine dye primers (Fig. 3, A and C) (*3*). The combination of these four BODIPY dye primers yielded high-quality sequencing data when analyzed with mobility software correction; however, the spacing pattern of the BODIPY dye primer set was further improved in the beginning of the sequencing run when no software correction was applied at all (*4*). Further evaluation of other BODIPY-linker combinations yielded an optimal dye primer set (*5*). Thus, a set of four BODIPY-linker constructs was identified that generated excellent sequence data when analyzed without mobility correction and gave an indistinguishable spacing pattern compared with software-corrected conventional sequencing reactions.

Comparison of normalized, overlapping emission spectra revealed that the bandwidths of the BODIPY dye primer set are narrower than their respective conventional dye primer counterparts (*6*), resulting in lower noise cross-talk between the instrument's collection filters (Fig. 4). The signal strength of BODIPY dyes, measured by fluorescence spectroscopy and an ABI 373A

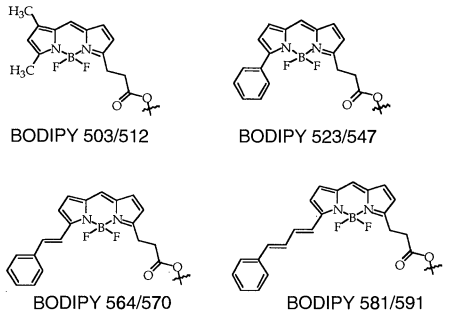

Fig. 1. Chemical structures of four BODIPY dyes for automated DNA sequencing. BODIPY dyes (4,4-difluoro-4-bora-3α,4α-diaza-*s*-indacene-3-propionic acid) are indicated followed by their approximate absorption/emission maxima. BODIPY 503/512 (5,7-dimethyl-BODIPY), BODIPY 523/547 (5-phenyl-BODIPY), BODIPY 564/570 (5-styryl-BODIPY), and BODIPY 581/591 [5-(4-phenyl-1,3-butadienyl)-BODIPY].

Department of Molecular and Human Genetics, Baylor College of Medicine, Houston, TX 77030, USA.

*To whom correspondence should be addressed.